Eur. Phys. J. D **6**, 185–192 (1999)

THE EUROPEAN PHYSICAL JOURNAL D
EDP Sciences

Ab initio structures and stabilities of helide cations: HeX^{n+} (X = B-Ne, Al-Ar and n = 1-3)

J.M. Hughes and E.I. von Nagy-Felsobuki[a]

Department of Chemistry, The University of Newcastle, Callaghan, NSW 2308, Australia

Received: 11 May 1998 / Received in final form: 2 September 1998

Abstract. The electronic structure and molecular properties of helides of the form HeX^{n+} (where X = B-Ne, Al-Ar and n = 1-3) were studied using the CCSD(T) method in conjunction with the series of correlation-consistent basis sets. The highest level of theory employed, the CCSD(T)_FC/cc-pVQZ model, was used to elucidate trends in bond lengths, dissociation energies and harmonic frequencies. The more highly charged species were found to have shorter bond lengths than the singly charged species. The ground states of the helide cations were often those with longer bond lengths when compared with the excited state ions.

PACS. 31.25.Nj Electron-correlation calculations for diatomic molecules – 36.40.Mr Spectroscopy and geometrical structure of clusters

1 Introduction

The unique properties of helium place extraordinary demands on any quantum mechanical model of the chemistry of helium [1]. For example, helium has the highest first ionization energy (IE) of any element (*e.g.*, 24.588 eV [2]) and so no other neutral element can withdraw electrons from it in order to form a chemical bond. The electron affinity of helium and other noble gases is virtually zero and so they do not accept electrons readily from any other neutral atoms or molecules. The static electric-dipole polarizability (which reflects the degree to which a potential binding partner can deform the electronic structure of an atom) has a relatively small size of value 0.205 Å^3 [3]. These physical properties suggests there is a reluctance of helium to partake or to undergo any chemical reaction with other neutral elements. However, they do not totally exclude helium from chemically binding.

Frenking, Koch and coworkers [4–12] have unravelled the bonding nature of singly and doubly charged helide cations as well as some neutral molecules containing helium. They found that the singly charged species in the ground state were van der Waals complexes which were stabilized by charged-induced interactions. For the excited states the binding partner became a stronger acceptor and so covalent bonding was thought to dominate, yielding relatively shorter bond lengths. On the other hand, all the doubly charged species were considered to have covalent bonds and so exhibited considerably shorter bond lengths when compared with the singly charged species. Species such as $HeBe^{2+}$, HeB^{2+} and HeC^{2+} were predicted to be stable towards dissociation, whereas HeN^{2+} and HeO^{2+} were predicted to be unstable (but nevertheless still had a minimum in the ground-state potential). The ground state of $HeLi^{2+}$, HeF^{2+} and $HeNe^{2+}$ were calculated to be purely repulsive. The *ab initio* models employed were Møller-Plesset perturbative methods at forth-order (MP4), including single, double, triple and quadruple excitations (*i.e.* MP4(SDTQ)) using the 6-311G(2df, 2pd) basis set. The optimizations of structural parameters were carried out at the second-order MP level of theory (MP2) using the 6-31G(d, p) basis set.

Using an alternative approach, Radom and coworkers [13,14] have employed qualitative MO theory to describe the trends in bonding and stability of highly charged HeC^{n+} (where $n = 1, 2, 3$) and $HeSi^{n+}$ (where $n = 1, 2, 3, 4$) ions. For helium carbide and helium silicate species, the equilibrium geometries were calculated at both the all-electron (AE) MP2_AE-6-31G* level of theory and using the frozen-core (FC) approximation within the quadratic configuration interaction ansatz involving single, doubles, with a perturbative treatment of triples excitations (*i.e.* QCISD(T)_FC/6-311G(MC)**). The ground-state helides showed significantly shorter bond lengths as the charge was increased. The trend in bonding was rationalized by the number of electrons occupying anti-bonding MOs that were interspersed between bonding and non-bonding MOs. Molecular charge also influenced the anti-bonding orbitals which led to finer variations in bond length.

There has been no systematic study encompassing a second-row sweep of charged helium diatomics of the form

---

[a] e-mail: `chvo@cc.newcastle.edu.au`

HeX^{n+} (where X = Al-Ar, $n = 1, 2, 3$) nor has there been a first-row sweep using high-quality *ab initio* theory (*i.e.* couple cluster with single, double excitations with a non-iterative perturbative inclusion of triple excitations - CCSD(T)). As an extension of our earlier work on the helide cations [15–20] we wish to report on the electronic structure (including stability, geometries, harmonic frequencies and dissociation energies) of the helide ions of form HeX^{n+} (where X = B-Ne, Al-Ar and $n = 1, 2$ and 3) using basis sets descending in quality from correlation-consistent polarized valence quadruple zeta (cc-pVQZ), aug-cc-pVTZ (augmented triple zeta), cc-pVTZ to cc-pVDZ (double zeta). The diatomic helides cations (*i.e.* He-X^{n+}, where X = B-Ne, Si and $n = 1, 2$) were specifically chosen so that comparisons could be made with *ab initio* calculations already undertaken by Frenking Koch and coworkers [10] and Radom and coworkers [14] using MP2_AE/6-31G(d, p) and QCISD(Y)_FC/6-311G(MC)** level of theory, respectively.

2 Computational procedure

Standard electronic *ab initio* calculations were performed using the Gaussian 94 suite of programmes [21]. The equilibrium geometries, harmonic frequencies and dissociation energies were determined for the ground and some excited states of the diatomic helide cations.

Electrons were correlated using the CCSD(T) level of theory. Essentially, the CCSD(T) method can provide accurate descriptions of molecular systems even when the SCF supplies a poor zeroth-order description. The CCSD(T) method for these species also allows use of large one-particle basis sets in order to achieve chemical accuracy. It therefore provides an appropriate compromise between accuracy and computational feasibility [22].

The unrestricted Hartree-Fock (UHF) wave function was used as the reference configuration for open-shell cations within the CCSD(T) ansatz, whereas the RHF wave function was used for closed-shell systems. Using the UHF method, the variational wave function is no longer an eigenfunction of the spin operator (S^2) with expectation value $S(S+1)$ [23]. However, examining the "before" and "after" spin annihilation effects for the open-shell cations revealed that the spin contamination was trivial in most cases and furthermore, the spin expectation values were correctly determined in all cases "after" the annihilation process.

Electronic calculations not only depend upon the level of electron correlation but also on the description of the one-particle basis set. Almlöff and Taylor [24] have noted that the basis functions optimized to describe electron correlation effects in atoms also described molecular correlation effects well. Dunning and coworkers [25–29] exploited this idea and developed the correlation-consistent family of basis sets. At the CCSD(T)_FC level of theory, Woon and Dunning [27] calculated the atomic polarizability of helium to be 1.362, 1.379 and 1.384 a_0^3 using the aug-cc-pVDZ, aug-cc-pVTZ and aug-cc-pVQZ basis sets, respectively. It should be noted that atomic polarizability is a severe test on the adequacy of a one-particle basis set. The triple and quadruple basis sets are in excellent agreement with the recommended value of 1.385 a_0^3 [30].

All geometry optimizations were performed using the default routines in Gaussian 94 (*i.e.* the analytical Berny routine for the HF methods and the numerical Fletcher-Powell routine for the CCSD(T) method) [21]. For geometry optimizations and single point energy calculations, the FC approximation was employed for the valence only basis sets, whereas the AE calculations were employed for the cc-pCVTZ basis set (which includes specific functions for core-core and core-valence electron correlation). For the sake of uniformity and completeness the structural parameter for the diatomic molecules were studied at the HF and CCSD(T)_FC/cc-pVXZ (where X = D, T and Q) level of theory and further supplemented by using the aug-cc-pVTZ basis set. All stationary points were characterized by examining the harmonic frequencies. The effect of adding core, diffuse and higher angular momentum functions to the basis was also examined.

3 Results and discussion

The quality of the basis set has a major bearing on the description of the helide ions. To ascertain the suitability of each basis set, HF and CCSD(T)_FC calculations were performed to determine the transition energy between the ground state and the first-excited state of helium and the first- and second-row elements. Table 1 gives the calculated HF and CCSD(T)_FC transition energies for the various correlation-consistent basis sets together with the experimental values [2]. It shows that none of the basis sets perform well at the HF level of theory (*e.g.* average error excluding helium is of the order ±1.5 eV) with the majority of the transition energies too large when compared with experiment (except for boron, carbon, aluminium and silicon where the calculated results are too small). The smallest basis set employed (*i.e.* the cc-pVDZ) performed poorly for helium, where an error of almost 100% occurred due to a lack of diffuse and polarization functions. A different trend is evident for the CCSD(T) results. Here the average error (which excludes the helium transition energy) is of order ±0.2 eV. The CCSD(T) error shows a general improvement from 0.28 eV to ±0.18 eV as the one-particle basis sets attains greater flexibility. One of the main factors contributing to the error is due to the excited D states of X^{n+}, which are poorly described using a single reference determinant. For helium, basis sets at triple and quadruple zeta augmented with diffuse functions almost mimic the experimental separation. It should not be forgotten that these results employ the FC approximation, neglect core correlation and relativistic effects. Nevertheless, they do give some credence for high levels of theory at least at the triple zeta level of flexibility yielding reasonably accurate transition energies.

The optimum geometry of each of the He-X^{n+} (where X = B-Ne, Al-Ar and n = 1-3) ions were calculated using the four correlation-consistent basis sets at the

Table 1. Comparison of theoretical and experimental transition energies (in eV) between the ground and first-excited states of the first- and second-row main group elements using the correlation-consistent basis sets[a].

Ion	Transition	cc-pVDZ		cc-pVTZ		aug-cc-pVTZ		cc-pVQZ		aug-cc-pVQZ		Exp.
		HF	CCSD(T)	HF	CCSD(T)	HF	CCSD(T)	HF	CCSD(T)	HF	CCSD(T)	
He	${}^1\mathrm{S} \rightarrow {}^3\mathrm{S}$	39.57	40.45	25.19	26.23	18.83	19.88	22.90	23.98	18.78	19.86	19.82
B^+	${}^1\mathrm{S} \rightarrow {}^3\mathrm{P}$	3.18	4.69	3.15	4.65	3.15	4.65	3.13	4.65	3.13	4.65	4.63
C^+	${}^2\mathrm{P} \rightarrow {}^4\mathrm{P}$	3.71	5.27	3.66	5.30	3.66	5.31	3.64	5.32	3.64	5.32	5.33
N^+	${}^3\mathrm{P} \rightarrow {}^3\mathrm{D}$	12.41	11.79	12.33	11.59	8.94	9.48	12.31	11.56	12.34	11.55	11.44
O^+	${}^4\mathrm{S} \rightarrow {}^2\mathrm{D}$	4.99	3.75	4.97	3.65	4.96	3.64	4.97	3.61	4.97	3.60	3.32
F^+	${}^3\mathrm{P} \rightarrow {}^1\mathrm{D}$	4.35	2.85	4.40	2.81	4.39	2.80	4.41	2.78	4.41	2.78	2.59
Ne^{2+}	${}^3\mathrm{P} \rightarrow {}^1\mathrm{D}$	5.28	3.46	5.31	3.39	5.31	3.38	5.32	3.36	5.32	3.36	3.20
Al^+	${}^1\mathrm{S} \rightarrow {}^3\mathrm{P}$	3.57	4.52	3.55	4.52	3.54	4.51	3.52	4.49	3.51	4.49	4.64
Si^+	${}^2\mathrm{P} \rightarrow {}^4\mathrm{P}$	3.91	5.07	3.89	5.11	3.88	5.10	3.87	5.11	3.87	5.11	5.47
P^+	${}^3\mathrm{P} \rightarrow {}^3\mathrm{D}$	9.18	8.48	9.25	8.43	9.25	8.42	9.27	8.39	9.27	8.39	8.09
S^+	${}^4\mathrm{S} \rightarrow {}^2\mathrm{D}$	3.01	2.33	2.97	2.16	2.97	2.15	2.97	2.11	2.97	2.10	1.84
Cl^+	${}^3\mathrm{P} \rightarrow {}^1\mathrm{D}$	2.73	1.73	2.73	1.73	2.74	1.73	2.78	1.60	2.78	1.60	1.44
Ar^{2+}	${}^3\mathrm{P} \rightarrow {}^1\mathrm{D}$	3.19	2.02	3.22	1.92	3.22	1.91	3.22	1.88	3.22	1.88	1.74
Error[b]		±1.41	±0.28	±1.45	±0.21	±1.58	±0.36	±1.46	±0.18	±1.46	±0.18	

[a] The experimental values are taken from Moore [2].

[b] The error is determined as the average of the differences between the calculated and experimental separations for the first- and second-row elements. The helium state separation is not included in the error analysis.

HF and CCSD(T)_FC levels of theory. Table 2 gives the optimal He-X interarmonic distances for the ground and some excited states for ions containing first- and second-row elements calculated using only the highest level of theory available in this investigation (*i.e.* the CCSD(T)_FC/cc-pVQZ model), with the results for the other three particle basis sets available on request. The geometries calculated by Frenking, Koch and coworkers [10] and Radom and coworkers [14] using MP2_AE/6-31G(d,p) and QCISD(T)_FC/6-311G(M)** level of theory, respectively, are also given in the table (where such comparisons can be made). The basis set superposition error (BSSE) was calculated using the counterpoise method for both the HF and CCSD(T) models and was found to be relatively flat near the potential energy minima (see below).

There is generally a "good" agreement between the Frenking, Koch and coworkers [10] and the CCSD(T)_FC results particularly for the cc-pVDZ basis sets, although this is expected since the quality of both basis sets are of double zeta quality. The greatest variation in interatomic distances occurs for the singly charged ions with long bond lengths. For the CCSD(T)_FC/cc-pVQZ model the interatomic distances are smaller by up to 0.2 Å when compared with the MP results [10]. Unlike the singly charged species, the doubly charged ions exhibit a general bond lengthening when compared with the MP results [10], although the variation is an order of magnitude less (*i.e.* between 0.02 and 0.05 Å).

Radom and coworkers [14] using the QCISD(T)_FC/6-311G(MC)** level of theory calculated bond lengths of $(\mathrm{X}^2\Pi)$ HeC$^+$, $({}^4\Sigma^-)$ HeC$^+$, $(\mathrm{X}^1\Sigma^+)$ HeC^{2+}, $({}^3\Pi)$ HeC^{2+} and $(\mathrm{X}^2\Sigma^+)$ HeC^{3+} to be 2.504, 1.177, 1.522, 1.186 and 1.310 Å, respectively. Compared with the CCSD(T)_FC/cc-pVQZ, the absolute differences in the bond lengths are 0.3, 0.02, 0.02, 0.008 and 0.04 Å, respectively. Similar sized differences are observed for ions containing second-row atoms; for example, for $(\mathrm{X}^2\Pi)$ HeSi$^+$, $({}^4\Sigma^-)$ HeSi$^+$, $(\mathrm{X}^1\Sigma^+)$ HeSi^{2+}, $({}^3\Pi)$ HeSi^{2+} and $(\mathrm{X}^2\Sigma^+)$ HeSi^{3+} the differences in bond lengths are 0.4, 0.05, 0.2, 0.02 and 0.03 Å, respectively.

The bond length for all ions studied systematically decreased as the basis set quality improved from cc-pVDZ to cc-pVQZ. This result is not unexpected since it is well known that the correlation-consistent basis sets display a monotonic convergence as the basis set quality is systematically improved [25,31–34]. The effect of electron correlation is more pronounced for the ground electronic states of the singly charged species where the variation in bond length usually decreases by up to 0.5 Å. For example, the $\mathrm{X}^3\Sigma^-$ electronic state of HeN$^+$ has a bond shortening of ~ 0.4 Å. In contrast, there is far less variation (by an order of magnitude) caused by electron correlation for the more highly charged species as well as for the excited states of the singly charged species. In essence, electron correlation appears more important for those ions that have relatively long bond lengths compared with those that exhibit relatively shorter bond lengths of ~ 1.1 to 1.3 Å in size. As would be expected there is more variation between the HF and CCSD(T) models for the helium ions containing second-row elements compared with those containing the first-row atoms.

The short bond lengths for the helide cations raises concerns about whether their magnitude is due to the

Table 2. The optimized bond lengths (R_e), total energy, zero-point energy (ZPE) and harmonic frequencies (ω_1) of the diatomic helides of form He-X^{n+} (where X = B-Ne, Al-Ar) determined at the CCSD(T)_FC/cc-pVQZ level of theory.

Ion	State	R_e		Energy	ZPE	ω_1
		[a] Lit (/Å)	This Work (/Å)	(/E_h)	(/kJ mol^{-1})	(/cm^{-1})
HeB$^+$	$X^1\Sigma^+$	2.912	2.7891	−27.201779	0.57	96.75
HeB$^+$	$^3\Pi$	1.454	1.4064	−27.040722	3.53	589.87
HeC$^+$	$X^2\Pi$	2.406 (2.504)	2.2330	−40.279721	1.46	243.70
HeC$^+$	$^4\Sigma^-$	1.168 (1.177)	1.1555	−40.131576	7.78	1334.53
HeN$^+$	$^1\Sigma^-$	—	1.5341	−56.827606	2.85	476.70
HeN$^+$	$X^3\Sigma^-$	1.749	1.5545	−56.904280	2.73	456.23
HeO$^+$	$^2\Pi$	1.191	1.1908	−77.295245	6.44	1076.43
HeO$^+$	$X^4\Sigma^-$	2.473	2.3773	−77.402966	8.84	147.83
HeF$^+$	$^1\Sigma^+$	1.024	1.0295	−101.905378	9.89	1653.91
HeF$^+$	$X^3\Pi$	2.123	1.9570	−101.921709	1.54	257.85
HeNe$^+$	$X^2\Sigma^+$	1.406	1.4317	−130.983415	5.51	920.84
HeNe$^+$	$^4\Sigma^+$	—	2.6655	−130.119071	3.56	594.57
HeB^{2+}	$X^2\Sigma^+$	1.339	1.3531	−26.323036	5.81	971.68
HeC^{2+}	$X^1\Sigma^+$	1.575 (1.522)	1.5437	−39.416250	4.52	755.94
HeC^{2+}	$^3\Pi$	1.167 (1.186)	1.1776	−39.255801	8.66	1448.15
HeN^{2+}	$X^2\Pi$	1.321	1.3258	−55.891800	6.69	1118.91
HeN^{2+}	$^4\Sigma^-$	1.060	1.0699	−55.760134	1.08	1801.12
HeO^{2+}	$^1\Sigma^-$	—	1.1982	−76.177112	7.91	1321.82
HeO^{2+}	$X^3\Sigma^-$	1.164	1.2088	−76.276347	7.76	1297.51
HeF^{2+}	$^2\Pi$	1.044	1.1149	−100.727863	8.15	1362.36
HeNe^{2+}	$^1\Sigma^+$	1.025	1.0567	−129.734069	7.70	1285.29
HeB^{3+}	$X^1\Sigma^+$	—	1.2447	−25.045792	8.90	1488.53
HeC^{3+}	$X^2\Sigma^+$	(1.310)	1.3531	−37.868511	4.00	668.59
HeAl$^+$	$X^1\Sigma^+$	—	3.4548	−244.617556	0.31	51.85
HeAl$^+$	$^3\Pi$	—	2.2335	−244.454485	0.96	160.85
HeSi$^+$	$X^2\Pi$	(2.437)	2.7991	−291.542570	0.64	106.98
HeSi$^+$	$^4\Sigma^-$	(1.757)	1.7056	−291.366981	3.33	556.90
HeP$^+$	$^1\Sigma^-$	—	2.4595	−343.303906	0.68	114.19
HeP$^+$	$X^3\Sigma^-$	—	2.2718	−343.347851	1.13	189.75
HeS$^+$	$^2\Pi$	—	2.4637	−400.117988	0.78	130.38
HeS$^+$	$X^4\Sigma^-$	—	3.1289	−400.194880	0.39	65.80
HeCl$^+$	$^1\Sigma^+$	—	1.5171	−462.080890	4.27	714.15
HeCl$^+$	$X^3\Pi$	—	2.7698	−462.125088	0.54	89.70
HeAr$^+$	$X^2\Sigma^+$	—	2.4284	−529.401729	0.96	159.73
HeAr$^+$	$^4\Sigma^+$	—	1.9943	−528.749507	0.36	360.43
HeAl^{2+}	$X^2\Sigma^+$	—	2.0579	−243.940659	1.85	309.11
HeSi^{2+}	$X^1\Sigma^+$	(2.437)	2.2992	−290.949273	1.58	260.49
HeSi^{2+}	$^3\Pi$	(1.714)	1.6951	−290.735274	4.01	670.68
HeP^{2+}	$X^2\Pi$	—	1.9031	−342.634996	2.77	462.57
HeP^{2+}	$^4\Sigma^-$	—	1.5097	−342.427307	6.05	1012.11
HeS^{2+}	$^1\Sigma^-$	—	1.6442	−399.313827	4.34	724.68
HeS^{2+}	$X^3\Sigma^-$	—	1.6467	−399.369152	4.43	740.58
HeCl^{2+}	$^2\Pi$	—	1.4836	−461.213908	5.97	997.52
HeCl^{2+}	$X^4\Sigma^-$	—	2.1911	−461.262779	2.06	344.19
HeAr^{2+}	$X^1\Sigma^+$	—	1.3662	−528.418295	7.52	1258.15
HeAr^{2+}	$^3\Pi$	—	1.8867	−528.409489	3.63	607.18
HeAl^{3+}	$X^1\Sigma^+$	—	1.6725	−242.949298	4.92	822.72
HeSi^{3+}	$X^2\Sigma^+$	(1.693)	1.6898	−289.773495	4.74	792.18
HeP^{3+}	$X^1\Sigma^+$	—	1.7752	−341.557879	4.33	723.41
HeP^{3+}	$^3\Pi$	—	1.5430	−341.309864	6.08	1016.25
HeS^{3+}	$X^2\Pi$	—	1.6121	−398.138151	5.59	933.94
HeS^{3+}	$^4\Sigma^-$	—	1.4607	−397.908841	6.06	1013.23
HeCl^{3+}	$^1\Sigma^-$	—	1.5088	−489.866894	6.30	1052.26
HeCl^{3+}	$X^3\Sigma^-$	—	1.5165	−489.933000	6.09	1018.73

[a] Values without brackets were calculated by Frenking, Koch and coworkers [10] at the MP2_AE/6-31G(d,p) level of theory. Values in brackets were calculated by Radom and coworkers [14] at the QCISD(T)_FC/6-311G(MC)** level of theory.

inadequacy of the basis sets employed (and in particular the number of polarization functions), the reliance on a single reference wavefunction (*i.e.* lack of a multi-reference effects) or an artefact of the FC approximation.

In the case of $(X^3\Sigma^-)$ HeN^+ the difference between the HF and CCSD(T) bond length using cc-pVDZ, cc-pCTZ and cc-pVQZ basis sets is 0.304, 0.324 and 0.356 Å, respectively. This bond shortening is generally reflected across the series. In fact the general rule-of-thumb for both models is that increasing the flexibility of the basis set shortens the bond length.

We have performed preliminary CASSCF calculations on $(X^3\Sigma^-)$ HeN^+. The calculations indicated that there were few important configurations and that these do not account for the dramatic decrease in bond length. Moreover, Gu, Buenker, Hirsch and Kimura [33] have recently employed a multi-reference double configuration interaction (MRD-CI) using a relatively large helium and nitrogen basis of $(9s, 4p, 1d)/[7s, 3p, 1d]$ and $(13s, 8p, 2d)/[7s, 4p, 2d]$, respectively. They found that the equilibrium bond distance for the ground state of HeN^+ was 1.618 Å. The CCSD(T)_AE/cc-pCVTZ model obtained a value 0.052 Å shorter than this result, whereas the corresponding value at the MP2_AE/6-31G(d, p) level was longer by 0.172 Å. Similar variations would be anticipated for the other helide cations given in Table 2.

The optimized bond length for $(X^3\Sigma^-)$ HeN^+ at the MP2_FC/6-31G(d, p) and MP2_AE/6-31G(d, p) level of theory is 1.899 and 1.749 Å, respectively. That is, the FC approximation significantly lengthens the bond by 0.150 Å. On the other hand, using the cc-pCVTZ basis set, the MP2_FC and MP2_AE calculations predict bond lengths of 1.597 and 1.595 Å, respectively. The bond length difference is only 0.002 Å. The CCSD(T)_AE/cc-pCVTZ and CCSD(T)_FC/cc-pCVTZ models yield bond lengths of 1.566 and 1.568 Å, respectively. That is, in general, invoking the FC approximation does nor cause short bond lengths.

Stationary points found on the potential energy surface for all the first- and second-row helides were characterized by determining the harmonic frequencies to ensure the points were local minima. At the CCSD(T)_FC level of theory the harmonic frequencies were determined by using double numerical differentiation techniques. Table 2 gives the total energies, zero-point energies and harmonic frequencies for the ground and some excited states of the helide cations. No imaginary frequencies were found. Generally, the HF harmonic frequencies compared with the CCSD(T) result, particularly for the species with longer bond lengths. The higher frequencies correspond to those ions that are either highly charged or which have rather short bond lengths. The harmonic frequencies are not amenable to a correction factor nor is it possible to determine the frequencies using a basis set limit criterion since there is no apparent trend in frequencies across the series as a function of basis set size.

To unravel the bonding trends in the diatomic helides it is useful to compare the interatomic distances across the helide series [10]. Figures 1(a) and 1(b) illustrate the comparisons not only with respect to increasing atomic number of the acceptor ion X, but also with respect to increasing molecular charge for helides containing the first- and second-row atoms, respectively. Figure 1(a) matches the analysis of Frenking, Koch and coworkers [10] for the singly charged helide cations containing first-row atoms. In Figure 1(a) the discontinuity in the doubly charged ions is due to the ground states of HeF^{2+} and $HeNe^{2+}$ not being bound. For the triple charged HeX^{3+} ions (where X = N, O, F and Ne) it was found that the electrostatic repulsion was dominant and, as a consequence, no stable structures were found for these ions. In contrast to this, Figure 1(b) shows that only the $HeAr^{3+}$ ground state is not bound. This is not surprising since the ground state of $HeAr^{2+}$ already has a very short bond length of 1.3662 Å. The shortest overall bond length for the entire series is that of the excited $^1\Sigma^+$ of HeF^+ ion with an equilibrium He-F bond length of 1.0295 Å. Furthermore, the bond length trends for helides containing first- and second-row elements are similar (where comparisons can be made) and moreover, are consistent with both the donor-acceptor model of Frenking, Koch and coworkers [10] and the MO occupation model of Radom and coworkers [14,35,36].

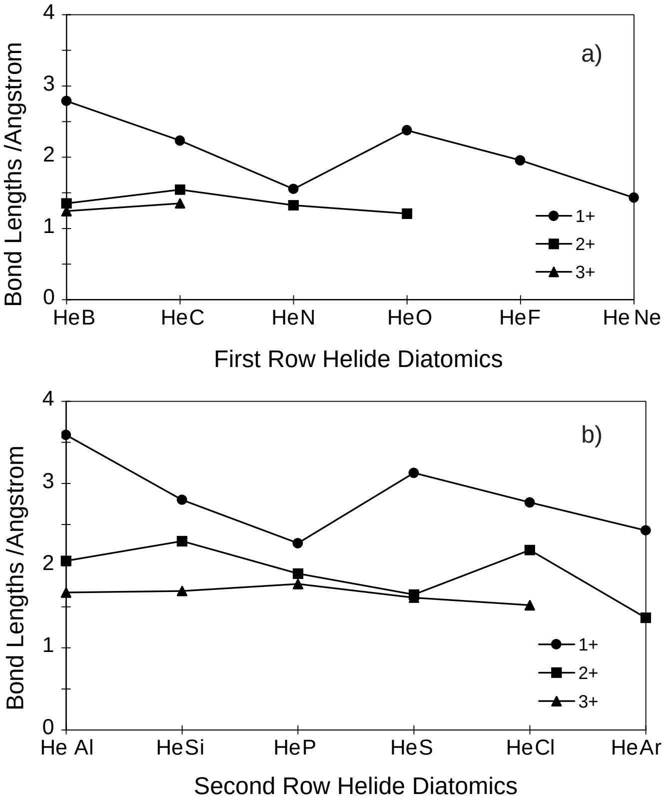

Fig. 1. (a) The variation of bond lengths (in Å) at the CCSD(T)_FC/cc-pVQZ level of theory for the electronic ground states of the helides He-X^{n+} (where X = B-Ne and n = 1-3) with respect to increasing atomic number and charge. (b) The variation of bond lengths (in Å) at the CCSD(T)_FC/cc-pVQZ level of theory for the electronic ground states of the helides He-X^{n+} (where X = Al-Ar and n = 1-3) with respect to increasing atomic number and charge.

Table 3. The CCSD(T)_FC dissociation energies and BSSE (the values in brackets indicate HF BSSE) for the ground and selected excited states of HeX^{n+} (where X = B-Ne and n = 1-3) in kJ mol^{-1}.

Dissociation Reaction	cc-pVDZ		cc-pVTZ		aug-cc-pVTZ		cc-pVQZ		F&K(b)
	D_0	BSSE	D_0	BSSE	D_0	BSSE	D_0	BSSE	
$\mathrm{HeB^{+}}(\chi^{1}\Sigma^{+}) \rightarrow \mathrm{He}(^{1}\mathrm{S}) + \mathrm{B^{+}}(^{1}\mathrm{S})$	+2.35	0.8 (0.5)	+1.72	0.1 (0.04)	+1.49	0.06 (0.008)	+2.71	0.05 (0.01)	+1.67
$\mathrm{HeB^{+}}(^{3}\Pi) \rightarrow \mathrm{He}(^{1}\mathrm{S}) + \mathrm{B^{+}}(^{3}\mathrm{P})$	+17.52	2.5 (1.0)	+29.25	0.5 (0.09)	+23.27	0.3 (0.08)	+28.25	0.2 (0.04)	+20.92
$\mathrm{HeC^{+}}(\chi^{2}\Pi) \rightarrow \mathrm{He}(^{1}\mathrm{S}) + \mathrm{C^{+}}(^{2}\mathrm{P})$	+4.16	4.5 (1.0)	+4.60	0.2 (0.04)	+4.29	0.1 (0.01)	+5.02	0.06 (0.02)	+3.77
$\mathrm{HeC^{+}}(^{4}\Sigma^{-}) \rightarrow \mathrm{He}(^{1}\mathrm{S}) + \mathrm{C^{+}}(^{4}\mathrm{P})$	+116.13	0.3 (0.4)	+132.55	0.7 (0.1)	+118.78	0.8 (0.06)	+137.58	0.3 (0.03)	+115.5
$\mathrm{HeN^{+}}(^{1}\Sigma^{-}) \rightarrow \mathrm{He}(^{1}\mathrm{S}) + \mathrm{N^{+}}(^{1}\mathrm{D})$	+11.40	1.9 (0.7)	+21.29	0.6 (0.09)	+56.65	0.5 (0.04)	+23.01	0.2 (0.02)	—
$\mathrm{HeN^{+}}(\chi^{3}\Sigma^{-}) \rightarrow \mathrm{He}(^{1}\mathrm{S}) + \mathrm{N^{+}}(^{3}\mathrm{P})$	+10.94	1.1 (0.4)	+22.64	0.4 (0.07)	+19.65	0.4 (0.03)	+24.68	0.2 (0.04)	+15.48
$\mathrm{HeO^{+}}(^{2}\Pi) \rightarrow \mathrm{He}(^{1}\mathrm{S}) + \mathrm{O^{+}}(^{2}\mathrm{D})$	+33.68	4.1 (1.1)	+65.73	1.6 (0.2)	+58.62	0.5 (0.07)	+72.74	0.6 (0.04)	+2.51
$\mathrm{HeO^{+}}(\chi^{4}\Sigma^{-}) \rightarrow \mathrm{He}(^{1}\mathrm{S}) + \mathrm{O^{+}}(^{4}\mathrm{S})$	+1.92	0.4 (0.2)	+2.77	0.1 (0.09)	+2.96	0.1 (0.05)	+2.27	0.06 (0.03)	+7.53
$\mathrm{HeF^{+}}(^{1}\Sigma^{+}) \rightarrow \mathrm{He}(^{1}\mathrm{S}) + \mathrm{F^{+}}(^{1}\mathrm{D})$	+279.33	5.3 (1.1)	+230.80	2.4 (0.3)	—(a)	—	+238.66	0.4 (0.08)	+188.70
$\mathrm{HeF^{+}}(\chi^{3}\Pi) \rightarrow \mathrm{He}(^{1}\mathrm{S}) + \mathrm{F^{+}}(^{3}\mathrm{P})$	+3.89	0.5 (0.4)	+6.23	0.3 (0.2)	+10.50	0.7 (0.1)	+5.05	0.06 (0.06)	+5.02
$\mathrm{HeNe^{+}}(\chi^{2}\Sigma^{+}) \rightarrow \mathrm{He}(^{1}\mathrm{S}) + \mathrm{Ne^{+}}(^{2}\mathrm{P})$	+46.11	0.6 (0.2)	+59.81	0.6 (0.5)	+56.65	0.8 (0.5)	+65.06	0.2 (0.2)	+38.07
$\mathrm{HeB^{2+}}(\chi^{2}\Sigma^{+}) \rightarrow \mathrm{He^{+}}(^{2}\mathrm{S}) + \mathrm{B^{+}}(^{1}\mathrm{S})$	+35.25	2.2 (2.1)	+67.67	0.2 (0.1)	+57.24	0.6 (0.2)	+58.79	0.04 (0.02)	+63.60
$\mathrm{HeC^{2+}}(\chi^{1}\Sigma^{+}) \rightarrow \mathrm{He}(^{1}\mathrm{S}) + \mathrm{C^{2+}}(^{1}\mathrm{S})$	+61.28	2.2 (0.6)	+82.30	0.3 (0.05)	+74.69	0.3 (0.02)	+85.24	0.04 (0.02)	+70.28
$\mathrm{HeC^{2+}}(^{3}\Pi) \rightarrow \mathrm{He^{+}}(^{2}\mathrm{S}) + \mathrm{C^{+}}(^{2}\mathrm{P})$	−330.24	3.5 (2.5)	−307.28	0.8 (0.2)	−324.02	0.3 (0.02)	−322.44	0.3 (0.01)	−318.82
$\mathrm{HeN^{2+}}(\chi^{2}\Pi) \rightarrow \mathrm{He^{+}}(^{2}\mathrm{S}) + \mathrm{N^{+}}(^{3}\mathrm{P})$	−298.06	2.2 (1.6)	−261.54	0.7 (0.2)	−259.57	0.7 (0.04)	−273.40	0.2 (0.02)	−291.62
$\mathrm{HeN^{2+}}(^{4}\Sigma^{-}) \rightarrow \mathrm{He^{+}}(^{2}\mathrm{S}) + \mathrm{N^{+}}(^{3}\mathrm{P})$	−635.96	2.9 (2.3)	−708.90	0.6 (0.1)	−623.37	0.4 (0.02)	−623.17	0.3 (0.03)	−622.60
$\mathrm{HeO^{2+}}(^{1}\Sigma^{-}) \rightarrow \mathrm{He^{+}}(^{2}\mathrm{S}) + \mathrm{O^{+}}(^{2}\mathrm{D})$	−523.46	3.5 (1.6)	−491.61	1.3 (0.2)	−489.95	1.5 (0.3)	−507.65	0.5 (0.04)	—
$\mathrm{HeO^{2+}}(\chi^{3}\Sigma^{-}) \rightarrow \mathrm{He^{+}}(^{2}\mathrm{S}) + \mathrm{O^{+}}(^{4}\mathrm{S})$	−620.40	3.1 (0.8)	−581.14	1.3(0.4)	−505.07	1.5 (0.3)	−594.70	0.5 (0.04)	−623.41
$\mathrm{HeF^{2+}}(^{2}\Pi) \rightarrow \mathrm{He^{+}}(^{2}\mathrm{S}) + \mathrm{F^{+}}(^{2}\mathrm{D})$	−526.21	3.3 (1.3)	−753.96	1.6 (0.4)	−594.04	1.5 (1.0)	−769.47	0.6 (0.2)	−809.60
$\mathrm{HeNe^{2+}}(^{1}\Sigma^{+}) \rightarrow \mathrm{He^{+}}(^{2}\mathrm{S}) + \mathrm{Ne^{+}}(^{2}\mathrm{P})$	−901.88	5.6 (2.6)	−847.59	2.3(1.0)	−841.41	1.6 (1.1)	−840.80	0.8 (0.2)	−885.75
$\mathrm{HeB^{3+}}(\chi^{1}\Sigma^{+}) \rightarrow \mathrm{He^{+}}(^{2}\mathrm{S}) + \mathrm{B^{2+}}(^{1}\mathrm{S})$	−896.23	3.0 (2.9)	−863.39	0.2 (0.1)	−879.43	0.3 (0.2)	−857.61	0.02 (0.01)	—
$\mathrm{HeC^{3+}}(\chi^{2}\Sigma^{+}) \rightarrow \mathrm{He^{+}}(^{2}\mathrm{S}) + \mathrm{C^{2+}}(^{1}\mathrm{S})$	—(a)	—	−1612.5	0.3 (0.1)	—(a)	—	−1609.3	0.04 (0.02)	—
$\mathrm{HeAl^{+}}(\chi^{1}\Sigma^{+}) \rightarrow \mathrm{He}(^{1}\mathrm{S}) + \mathrm{Al^{+}}(^{1}\mathrm{S})$	+0.81	0.7 (0.6)	+0.87	0.07 (0.04)	—(a)	—	+1.12	0.04 (0.02)	—
$\mathrm{HeAl^{+}}(^{3}\Sigma^{-}) \rightarrow \mathrm{He}(^{1}\mathrm{S}) + \mathrm{Al^{+}}(^{3}\mathrm{P})$	+2.95	1.3 (0.8)	+4.90	0.3 (0.07)	+6.46	0.4 (0.03)	+6.59	0.1 (0.03)	—
$\mathrm{HeSi^{+}}(\chi^{2}\Pi) \rightarrow \mathrm{He}(^{1}\mathrm{S}) + \mathrm{Si^{+}}(^{2}\mathrm{P})$	+1.53	0.8 (0.5)	+2.04	0.1 (0.04)	+3.30	0.07 (0.005)	+3.00	0.06 (0.02)	—
$\mathrm{HeSi^{+}}(^{4}\Sigma^{-}) \rightarrow \mathrm{He}(^{1}\mathrm{S}) + \mathrm{Si^{+}}(^{4}\mathrm{P})$	+18.18	2.4 (1.2)	+34.31	0.3 (0.1)	+36.07	0.4 (0.1)	+37.49	0.2 (0.03)	—
$\mathrm{HeP^{+}}(^{1}\Sigma^{-}) \rightarrow \mathrm{He}(^{1}\mathrm{S}) + \mathrm{P^{+}}(^{1}\mathrm{D})$	+1.53	0.8 (0.5)	+2.41	0.2 (0.04)	+4.31	0.02 (0.005)	+4.01	0.09 (0.01)	—
$\mathrm{HeP^{+}}(\chi^{3}\Sigma^{-}) \rightarrow \mathrm{He}(^{1}\mathrm{S}) + \mathrm{P^{+}}(^{3}\mathrm{P})$	+3.03	0.9 (0.6)	+5.37	0.3 (0.07)	—(a)	—	+7.74	0.09 (0.01)	—
$\mathrm{HeS^{+}}(^{2}\Pi) \rightarrow \mathrm{He}(^{1}\mathrm{S}) + \mathrm{S^{+}}(^{2}\mathrm{D})$	+0.47	0.4 (0.3)	+1.42	0.1 (0.04)	+3.48	0.3 (0.004)	+2.87	0.03 (0.02)	—
$\mathrm{HeS^{+}}(\chi^{4}\Sigma^{-}) \rightarrow \mathrm{He}(^{1}\mathrm{S}) + \mathrm{S^{+}}(^{4}\mathrm{S})$	+0.23	0.3 (0.3)	+1.19	0.1 (0.07)	+2.13	0.2 (0.03)	+1.18	0.04 (0.009)	—
$\mathrm{HeCl^{+}}(^{1}\Sigma^{+}) \rightarrow \mathrm{He}(^{1}\mathrm{S}) + \mathrm{Cl^{+}}(^{1}\mathrm{D})$	+5.14	2.7 (0.8)	+36.40	0.3 (0.2)	+37.13	1.1 (0.06)	+41.20	0.5 (0.04)	—
$\mathrm{HeCl^{+}}(\chi^{3}\Pi) \rightarrow \mathrm{He}(^{1}\mathrm{S}) + \mathrm{Cl^{+}}(^{3}\mathrm{P})$	+0.57	0.5 (0.3)	+1.55	0.1 (0.05)	+2.68	0.1 (0.003)	+2.49	0.06 (0.009)	—
$\mathrm{HeAr^{+}}(\chi^{2}\Sigma^{+}) \rightarrow \mathrm{He}(^{1}\mathrm{S}) + \mathrm{Ar^{+}}(^{2}\mathrm{P})$	+1.20	0.7 (0.4)	3.72	0.2 (0.07)	+4.64	0.3 (0.03)	+3.90	0.09 (0.03)	—
$\mathrm{HeAl^{2+}}(\chi^{2}\Sigma^{+}) \rightarrow \mathrm{He}(^{1}\mathrm{S}) + \mathrm{Al^{2+}}(^{2}\mathrm{S})$	+11.85	1.9 (1.1)	+19.95	0.3 (0.1)	+21.42	0.3 (0.03)	+22.32	0.09 (0.01)	—
$\mathrm{HeSi^{2+}}(\chi^{1}\Sigma^{+}) \rightarrow \mathrm{He}(^{1}\mathrm{S}) + \mathrm{Si^{2+}}(^{1}\mathrm{P})$	+7.42	1.1 (0.7)	+13.45	0.1(0.05)	+15.93	0.07 (0.007)	+16.07	0.09 (0.02)	—
$\mathrm{HeSi^{2+}}(^{3}\Pi) \rightarrow \mathrm{He}(^{1}\mathrm{S}) + \mathrm{Si^{2+}}(^{3}\mathrm{P})$	+46.53	2.5 (1.2)	+68.10	0.5 (0.08)	+69.42	0.4 (0.04)	+71.20	0.2 (0.03)	—
$\mathrm{HeP^{2+}}(\chi^{2}\Pi) \rightarrow \mathrm{He}(^{1}\mathrm{S}) + \mathrm{P^{2+}}(^{2}\mathrm{P})$	+19.85	1.5 (0.8)	+35.75	0.4 (0.06)	+26.20	0.3 (0.04)	+40.29	0.08 (0.05)	—
$\mathrm{HeP^{2+}}(^{4}\Sigma^{-}) \rightarrow \mathrm{He}(^{1}\mathrm{S}) + \mathrm{P^{2+}}(^{4}\mathrm{P})$	+116.79	2.4 (1.0)	+149.9	0.5 (0.09)	+151.73	0.3 (0.06)	+155.09	0.1 (0.05)	—
$\mathrm{HeS^{2+}}(^{1}\Sigma^{-}) \rightarrow \mathrm{He}(^{1}\mathrm{S}) + \mathrm{S^{2+}}(^{1}\mathrm{D})$	+53.87	2.4 (0.9)	+81.18	0.4(0.08)	+83.46	0.4 (0.03)	+84.99	0.2 (0.02)	—
$\mathrm{HeS^{2+}}(\chi^{3}\Sigma^{-}) \rightarrow \mathrm{He}(^{1}\mathrm{S}) + \mathrm{S^{2+}}(^{3}\mathrm{P})$	+54.34	2.0 (0.9)	+85.96	0.4(0.08)	+88.23	0.5 (0.04)	+90.88	0.2 (0.02)	—
$\mathrm{HeCl^{2+}}(^{2}\Pi) \rightarrow \mathrm{He}(^{1}\mathrm{S}) + \mathrm{Cl^{2+}}(^{2}\mathrm{D})$	+81.31	3.3 (1.0)	+130.81	0.3 (0.1)	+134.56	1.1 (0.06)	+140.89	0.1 (0.02)	—
$\mathrm{HeCl^{2+}}(\chi^{4}\Sigma^{-}) \rightarrow \mathrm{He}(^{1}\mathrm{S}) + \mathrm{Cl^{+}}(^{4}\mathrm{S})$	+8.09	1.1 (0.8)	+17.19	0.2 (0.1)	+21.17	0.2 (0.03)	+21.18	0.06 (0.04)	—
$\mathrm{HeAr^{2+}}(^{1}\Sigma^{+}) \rightarrow \mathrm{He^{+}}(^{2}\mathrm{S}) + \mathrm{Ar^{+}}(^{2}\mathrm{P})$	−258.68	2.7 (2.2)	−260.42	0.6(0.4)	−261.25	0.5 (0.2)	−264.99	0.05 (0.02)	—
$\mathrm{HeAr^{2+}}(\chi^{3}\Pi) \rightarrow \mathrm{He^{+}}(^{2}\mathrm{S}) + \mathrm{Ar^{+}}(^{2}\mathrm{P})$	−230.27	2.6 (2.1)	−258.13	0.6 (0.2)	−265.32	0.5 (0.2)	−227.56	0.04 (0.01)	—
$\mathrm{HeAl^{3+}}(\chi^{1}\Sigma^{+}) \rightarrow \mathrm{He^{+}}(^{2}\mathrm{S}) + \mathrm{Al^{2+}}(^{2}\mathrm{S})$	−260.90	1.6 (1.8)	−213.63	0.03 (0.05)	−212.14	0.2 (0.1)	−207.82	0.1 (0.004)	—
$\mathrm{HeSi^{3+}}(\chi^{2}\Sigma^{+}) \rightarrow \mathrm{He^{+}}(^{2}\mathrm{S}) + \mathrm{Si^{2+}}(^{1}\mathrm{P})$	−745.96	1.7 (1.6)	−703.33	0.06 (0.03)	−701.35	0.2 (0.1)	−697.72	0.1 (0.01)	—
$\mathrm{HeP^{3+}}(\chi^{1}\Sigma^{+}) \rightarrow \mathrm{He^{+}}(^{2}\mathrm{S}) + \mathrm{P^{2+}}(^{2}\mathrm{P})$	−451.26	1.4 (1.3)	−419.46	0.1(0.03)	−417.10	0.3 (0.1)	−416.08	0.2 (0.04)	—
$\mathrm{HeP^{3+}}(^{3}\Pi) \rightarrow \mathrm{He^{+}}(^{2}\mathrm{S}) + \mathrm{P^{2+}}(^{4}\mathrm{P})$	−459.26	1.7 (1.7)	−415.18	0.1 (0.08)	−413.31	0.3 (0.2)	−630.46	0.2 (0.04)	—
$\mathrm{HeS^{3+}}(\chi^{2}\Pi) \rightarrow \mathrm{He^{+}}(^{2}\mathrm{S}) + \mathrm{S^{2+}}(^{1}\mathrm{D})$	−649.77	2.0 (1.5)	−630.17	0.2 (0.07)	−628.75	0.4 (0.2)	−630.46	0.3 (0.009)	—
$\mathrm{HeS^{3+}}(^{4}\Sigma^{-}) \rightarrow \mathrm{He^{+}}(^{2}\mathrm{S}) + \mathrm{S^{2+}}(^{3}\mathrm{P})$	−1406.18	2.4 (1.8)	−1373.7	0.3 (0.1)	−1378.28	0.5 (0.2)	−1377.56	0.4 (0.01)	—
$\mathrm{HeCl^{3+}}(^{1}\Sigma^{-}) \rightarrow \mathrm{He^{+}}(^{2}\mathrm{S}) + \mathrm{Cl^{2+}}(^{2}\mathrm{D})$	−1072.44	2.9 (1.6)	−1028.5	0.5 (0.1)	−1026.82	1.1 (0.2)	−1025.33	0.3 (0.01)	—
$\mathrm{HeCl^{3+}}(\chi^{3}\Sigma^{-}) \rightarrow \mathrm{He^{+}}(^{2}\mathrm{S}) + \mathrm{Cl^{2+}}(^{4}\mathrm{S})$	−1146.73	2.8 (1.6)	−1101.1	0.5 (0.1)	−1086.00	1.1 (0.2)	−1096.08	0.4 (0.01)	—

(a) Local minima not found.

(b) Frenking, Koch and coworkers [10] using the MP4(SDQ)/6-311G(2*pd*, 2*df*)//MP2_AE/6-31G(*d*, *p*) level of theory.

The calculated dissociation energies D_0 and the respective BSSE for both the HF and CCSD(T) ansatz are given in Table 3 for the most favourable fragmentation pathways at the CCSD(T) level of theory. The HF dissociation energies are not given, since they were shown to be certainly inadequate with respect to the potential energy curves of many helide cations [10,37,38]. The HF BSSE are generally small (*i.e.* less than 1%) and in fact, much smaller than for the electron correlation model (which illustrates that the basis sets are at least saturated at the HF level).

The CCSD(T)_FC dissociation energies are compared with the results of Frenking, Koch and coworkers [10], which were determined using the MP2_AE/6-31G (*d*, *p*) // MP4 (SDTQ)_FC/6-3311G (2*pd*, 2*df*) method. Table 3 reveals that there is a wide discrepancy between the CCSD(T)_FC/cc-pVQZ results and those obtained at the MP level [10] for the singly charged species while there is far better agreement between the results obtained for the doubly charged species. For example, for the excited state of HeO^+ there is a discrepancy of almost 70 kJ mol^{-1} while the largest discrepancy for the doubly charged species occurs for the excited state of HeF^+ of 40 kJ mol^{-1}.

Lee and Scuseria [39] have noted that in many cases the CCSD(T)_FC/*spdfg* model compared exceptionally well with MRCI methods (often within chemical accuracy of ~ 4 kJ mol^{-1}) and that the agreement between the methods is not due to the result of fortuitous cancellations of higher-order contributions. Gu *et al.* [33] have recently determined the dissociation energy of HeN^+ ground state using MRCI methods where the D_e was calculated to be 16.91 kJ mol^{-1}, which is in excellent agreement with the CCSD(T)_FC/aug-cc-pVTZ result of 16.85 kJ mol^{-1} (a difference of only 0.06 kJ mol^{-1}). The CCSD(T)_FC/cc-p-VQZ model yields a value that was ~ 4 kJ mol^{-1} higher than the triple zeta result. The CCSD(T)_FC/cc-pVDZ value was underestimated by ~ 7 kJ mol^{-1} when compared with the MRCI value.

The CCSD(T) method must also be coupled with a sufficiently large basis set in order to reduce the BSSE. Table 3 reveals that BSSE contributes significantly to the overall dissociation energy for the cc-pVDZ basis set and hence this basis set should not be used for accurate calculation of D_0's. However, the BSSE was lowered by an order of magnitude as the basis set level increased from the double zeta to the quadruple zeta level.

All the He-X^+ species dissociated into neutral helium and X^+ due to the first IE of helium being higher than the respective first IE of the first- and second-row elements [2]. The heterolytic bond cleavage for the ground states of the singly charged species yields dissociation energies that are very small particularly for the second-row atoms, where most dissociation energies are below 7 kJ mol^{-1} (and endothermic). The rather low dissociation energies correspond to the relatively long bond lengths found for the ground states. On the other hand, the excited states exhibit significant bond shortening which correspond to an increase in dissociation energy. It is interesting to note that Frenking, Koch and coworkers [10] have found that the excited $^2\Pi$ state of HeO^+ had a surprisingly low D_0 value of 2.51 kJ mol^{-1} which does not correspond with the dissociation energy/bond length trend. However, the CCSD(T)_FC/aug-cc-pVTZ model yields a value of 58.62 kJ mol^{-1}, which does follow the dissociation energy/bond length trend.

For $HeNe^+$ a spectroscopic study is available for comparison. The experimental dissociation energy D_0 is 66.5 kJ mol^{-1} [40] which is in excellent agreement with the CCSD(T)_FC/cc-pVQZ result that predicts a value of 65.0 kJ mol^{-1}. This further highlights the accuracy of this *ab initio* method (*i.e.* the error is well below chemical accuracy of ~ 4 kJ mol^{-1}).

For $HeAl^+$, Niu and coworkers [41] have recently calculated the bond length and D_0 at the MP4(SDQ)_FC level of theory to be 3.44 Å and and 0.96 kJ mol^{-1}, respectively, which is in "excellent" agreement with the CCSD(T)_FC/cc-pVQZ result 3.45 Å and 1.12 kJ mol^{-1}, respectively. Using CASSCF, Hotokka and coworkers [42] have determined the D_0 and bond lengths of $HeAl^{3+}$ to be 114.8 kJ mol^{-1} (where the dissociation channel was $He + Al^{3+}$) and 1.67 Å, respectively, which is also in "excellent" agreement with the CCSD(T)/cc-pVQZ value of 118.4 kJ mol^{-1} and 1.67 Å, respectively.

For the doubly charged helides of the first row, only the dissociation of the ground states of HeB^{2+} and HeC^{2+} into $He^+ + B^+$ and $He + C^{2+}$, respectively, are found to be endothermic. All other excited and ground states of the first-row series dissociated into charged fragments and are exothermic. This is consistent with the results found by Frenking, Koch and coworkers [10]. In contrast to this, the majority of the second-row helide species (apart from $HeAr^{2+}$) dissociated *via* the $He + X^{2+}$ channel, and are endothermic reactions. The HeX^{2+} ions have also been calculated to have dissociation energies that are significantly larger than the HeX^+ species and as a consequence are potential candidates to be observed in the gas-phase. This may be particularly true for those excited ions that exhibit rather short bond lengths. All the triply charged species are found to dissociate via the charged-separation reaction of X^{2+} and He^+ and are exothermic reactions. Like the doubly charged species these highly charged helides exhibit even greater bond dissociation energy than their HeX^{2+} counterparts. For example, Wong and Radom [36] have studied $HeSi^{3+}$ and have found that the dissociation reaction is exothermic by 724 kJ mol^{-1} with a energy barrier of 100 kJ mol^{-1} determined at the MP4/6-311G(MC)($2d, 2p$) level of theory. The CCSD(T)_FC/cc-pVQZ yields a smaller D_0 value of 698 kJ mol^{-1}. The largest D_0 value (*i.e.* 1609 kJ mol^{-1}) determined is due to the dissociation of HeC^{3+} into He^+ and C^{2+}.

4 Conclusion

Helides of the form HeX^{n+} (where X = B-Ne, Al-Ar and n = 1-3) were studied using the CCSD(T) method in conjunction with the series of correlation-consistent basis sets. The highest level of theory employed, CCSD(T)_FC/cc-pVQZ, can be regarded as the most accurate predictor of molecular properties reported. The CCSD(T)_FC/cc-pVQZ model, was used to elucidate trends in bond lengths, dissociation energies and harmonic frequencies.

We would like to acknowledge the generous allocation of CPU time on the supercomputer facilities at ANU and the workstation facilities of the University of Newcastle. One of us (J.M.H.) wishes to acknowledge an Australian University of Newcastle Postgraduate Research award.

References

1. J. Wilkes, *Liquid and Solid Helium* (Clarendon, Oxford, 1967).
2. C.E. Moore, *Atom energy levels as derived from the analysis of optical spectra.* Nat. Stand Ref. Data Ser. Nat. Bur. Stand. (U.S.) NSRDS-NBS (1971).
3. T.M. Miller, B. Bederson, Adv. At. Mol. Phys. **13**, 1 (1977).
4. G. Frenking, D. Cremer, Struct. Bonding **73**, 17 (1990).
5. W. Koch, G. Frenking, J. Gauss, D. Cremer, J.R. Collins, J. Am. Chem. Soc. **109**, 5917 (1987).
6. W. Koch, G. Frenking, J. Chem. Soc. Chem. Commun. 1095 (1986).
7. W. Koch, G. Frenking, Int. J. Mass Spectrom. Ion Proc. **74**, 133 (1986).
8. W. Koch, J.R. Collins, G. Frenking, Chem. Phys. Lett. **132**, 330 (1986).
9. G. Frenking, W. Koch, J. Gauss, D. Cremer, J. Am. Chem. Soc. **110**, 8007 (1988).
10. G. Frenking, W. Koch, D. Cremer, J. Gauss, J.F. Liebman, J. Phys. Chem. **93**, 3397 (1989).
11. G. Frenking, W. Koch, J.F. Liebman, in *From Atoms to Polymers. Isoelectronic Analogies*, edited by J.F. Liebman, A. Greenberg (VCH Publishers, New York, 1989).
12. G. Frenking, W. Koch, F. Reichel, D. Cremer, J. Am. Chem. Soc. **112**, 4240 (1990).
13. M.W. Wong, L. Radom, J. Am. Chem. Soc. **110**, 2375 (1988).
14. E.D. Jemmis, M.W. Wong, H.-B. Bürgi, L. Radom, J. Mol. Struct. (Theochem.) **261**, 385 (1992).
15. J.M. Hughes, E.I. von Nagy-Felsobuki, Chem. Phys. **211**, 135 (1996).
16. J.M. Hughes, E.I. von Nagy-Felsobuki, J. Mol. Struct. (Theochem.) **389**, 1 (1997).
17. J.M. Hughes, E.I. von Nagy-Felsobuki, Phys. Chem. A **101**, 3995 (1997).
18. J.M. Hughes, E.I. von Nagy-Felsobuki, Chem. Phys. Lett. **272**, 313 (1997).
19. J.M. Hughes, E.I. von Nagy-Felsobuki, J. Mol. Struct. (Theochem.) **398**, 347 (1997).
20. J.M. Hughes, E.I. von Nagy-Felsobuki, Aust. J. Phys. **51**, 57 (1998).
21. M.J. Frisch, G.W. Trucks, H.B. Schlegel, P.M.W. Gill, B.G. Johnson, M.A. Robb, J.R. Cheeseman, T. Keith, G.A. Petersson, J.A. Montgomery, K. Raghavachari, M.A. Al-Lahim, V.G. Zakrzewski, J.V. Oritz, J.B. Foresman, J. Cioslowski, B.B. Stefanov, A. Nanayakkara, M. Challacombe, C.Y. Peng, P.Y. Ayala, W. Chen, M.W. Wong, J.L. Andres, E.S. Replogle, R. Gomperts, R.L. Martin, D.J. Fox, J.S. Binkley, D.J. Defrees, J. Baker, J.P. Stewart, M. Head-Gordon, C. Gonzalez, J.A. Pople, *Gaussian 94, Revision D.3* (Gaussian, Inc., Pittsburgh, 1995).
22. T.J. Lee, G.E. Scuseria, in *Quantum Mechanical Electronic Structure Calculations with Chemical Accuracy*, edited by S.R. Langhoff (Kluwer Academic, Boston, 1995).
23. T. Amos, L.C. Snyder, J. Chem. Phys. **41**, 1773 (1964).
24. J. Almlöff, P.R. Taylor, J. Chem. Phys. **86**, 4070 (1987).
25. T.H. Dunning Jr., J. Chem. Phys. **90**, 1007 (1989).
26. R.A. Kendell, T.H. Dunning Jr., R.J. Harrison, J. Chem. Phys. **96**, 6796 (1992).
27. D.E. Woon, T.H. Dunning Jr., J. Chem. Phys. **98**, 1358 (1993).
28. D.E. Woon, T.H. Dunning Jr., J. Chem. Phys. **100**, 2975 (1994).
29. D.E. Woon, T.H. Dunning Jr., J. Chem. Phys. **103**, 4572 (1995).
30. T.M. Miller, B. Bederson, Adv. At. Mol. Phys. **13**, 1 (1977).
31. P.R. Taylor, in *Lecture Notes in Quantum Chemistry*, edited by B.O. Roos (Springer-Verlag, Berlin, 1992) p. 406.
32. R.J. Bartlett, in *Modern Electronic Structure Theory*, Part 2, edited by D.R. Yarkony (World Scientific Publishing Co, Pty. Ltd, Singapore, 1995).
33. J.-P. Gu, R.J. Buenker, G. Hirsch, M. Kimura, J. Chem. Phys. **102**, 7540 (1995).
34. D.L. Cooper, S. Wilson, Mol. Phys. **44**, 161 (1981).
35. L. Radom, P.M.W. Gill, M.W. Wong, R. Nobes, Pure & Appl. Chem. **60**, 183 (1988).
36. M.W. Wong, L. Radom, J. Am. Chem. Soc. **110**, 2375 (1988).
37. R.W. Wetmore, R.J. LeRoy, R.K. Body, J. Phys. Chem. **88**, 6318 (1984).
38. R.W. Wetmore, R.J. LeRoy, R.K. Boyd, Chem. Phys. **89**, 329 (1984).
39. T.J. Lee, G.E. Scuseria, in *Quantum Mechanical Electronic Structure Calculations with Chemical Accuracy*, edited by S.R. Langhoff (Kluwer Academic, Boston, 1995).
40. I. Dabrowski, G. Herzberg, J. Mol. Spectrosc. **73**, 183 (1978).
41. J. Niu, B.K. Rao, O. Jena, M. Manninen, Phys. Rev. B **51**, 4475 (1995).
42. M. Hotokka, T. Kinstedt, P. Pykko, B.O. Roos, Mol. Phys. **52**, 23 (1984).